For better comprehension of mussel's thermal characteristics and their thermal effect on dynamic submarine electrical cables

Ziad Maksassi, Ahmed Ould El Moctar, Bertrand Garnier, Franck Schoefs, Emmanuel Schaeffer

For better comprehension of mussel's thermal characteristics and their thermal effect on dynamic submarine electrical cables

Ziad Maksassi[a,*], Ahmed Ould, E L Moctar[a], Bertrand Garnier[a], Franck Schoefs[b], Emmanuel Schaeffer[c]

[a] *Laboratoire de thermique et énergie de Nantes, LTeN, UMR CNRS 6607, Université de Nantes, Rue Christian Pauc, 44306 Nantes, France; ziad.maksassi@univ-nantes.fr, bertrand.garnier@univ-nantes.fr, ahmed.ouldelmoctar@univ-nantes.fr*

[b] *Institut de Recherche en Génie Civil et Mécanique, Univer-sité de Nantes, GeM, Rue de la Noë, 44321, Nantes, France; franck.schoefs@univ-nantes.fr*

[c] *Institut de Recherche en Énergie Électrique de Nantes-Atlantique, IREENA, EA 4642/IUML FR CNRS 3174, Université de Nantes, France; emmanuel.schaeffer@univ-nantes.fr*

* Correspondence: ziad.maksassi@univ-nantes.fr / maksassiziad@gmail.com

Abstract

Floating offshore wind turbines (FOWTs) face a major challenge when focusing on the effect of biofouling: biofouling by mussels on bottom-surface mobile connections, such as dynamic submarine electrical cables and mooring lines. Mussels are one of the dominant species in offshore wind farms in North Atlantic area. Amongst other effects, mussels can cause significant thermal impacts on dynamic power cables, which can lead to reduced performance or even failure. To address this issue, it is essential to thermally characterize mussels, including estimating their thermal resistance, so that they can be properly incorporated into the design and maintenance phases of the submarine dynamic power cables. This study investigates three key factors that could impact mussel thermal resistance, including mussel water filtering, imposed power during measurement, porosity (mussel's age). Results reveal that the thermal resistance of living mussels is smaller than that of dead mussels due to the metabolism phenomenon of water filtering. Additionally, thermal resistance decreases as mussel age (porosity) and imposed power during measurement increase. The results of this study offer novel insights into the thermal properties of mussels and their impact on submarine dynamic electrical cables used in FOWTs. The findings have practical implications for the design and maintenance of FOWTs, enhancing the sustainability of offshore wind energy production and provide a complete protocol for further investigations.

Keywords: dynamic power cable, biofouling, mussels, thermal characterization, effective thermal conductivity, marine renewable energy, floating offshore wind turbine

1. Introduction

In recent years, there has been a worldwide effort to advance floating wind turbine projects of

different magnitudes, spanning from prototype to pilot farm and commercial farm scales. An essential constituent of these initiatives is the dynamic submarine power cable (DSEC) that connects the wind turbines to static power cables on the sea bed, the latter being connected to the substation and the subaquatic energy network. Note that the substation can also be floating and that the dynamic power cable is shown to be a critical component [1]. Nevertheless, a notable challenge emerges owing to the fact that each project formulates its individual dynamic cable specifications, leading to a lack of standardization across the industry. As a result, the performance and reliability of dynamic cables become critical factors for the successful operation of floating wind turbine projects. The development of a universally-accepted set of technical specifications for dynamic power cables is imperative for the efficient and sustainable growth of the floating wind turbine industry.

The characteristics of dynamic cables for floating wind turbine projects are influenced by various factors. These include the unit power of the turbines, the general connection diagram, the architecture of the substations, the environmental conditions (water depth; wind, wave and current intensity and direction; biofouling) of the site, and the cable's design. For instance, the unit powers of pilot farms typically range between 6MW and 8MW, while commercial farms are expected to have unit powers of 12MW to 15MW by 2025. The general connection diagram may involve at least two cables per wind turbine connected in series or in parallel. The architecture of the substations may be integrated onto a wind turbine float or an independent float. Therefore, establishing dynamic cable specifications for floating wind turbine projects requires a comprehensive consideration of these factors.

Despite the unique needs of each farm, the most commonly used type of dynamic cable is the cross-linked polyethylene cable (XLPE), as shown in Figure 1. This cable pro-vides excellent electrical insulation. The XLPE cable has a high dielectric resistance, stable dielectric constant across all frequencies, and a low dielectric constant. However, despite the numerous advantages of XLPE cables, there are still several challenges associated with the dynamic cables used in floating wind turbines. These challenges include mechanical fatigue caused by the cable's continuous movement and exposure to the harsh marine environment, the accumulation of biofouling and its various effects [2] such as loading on mooring lines and cables [3,4,5,6], and the potential for damage due to fishing activities and other external factors. Therefore, developing durable and reliable dynamic cables is essential for the long-term success of floating wind turbine projects.

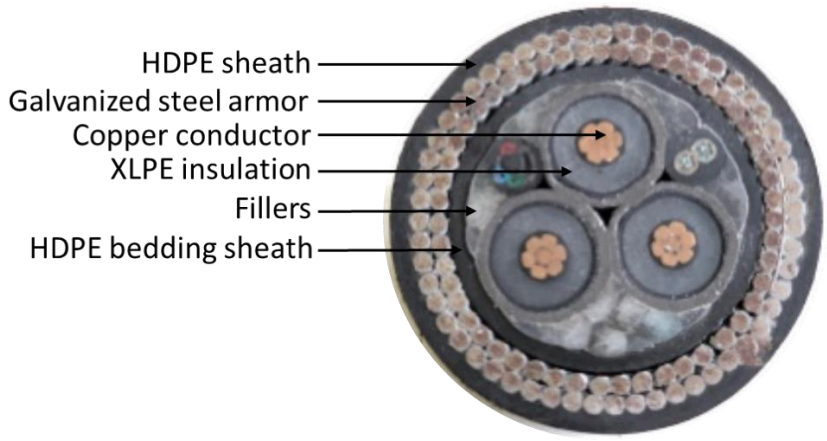

Figure 1. Cross-linked polyethylene (XLPE) insulation of dynamic power cable

Bio-colonization, the formation of inorganic and/or organic residues, has been documented to have significant impacts on the behavior of dynamic cables in floating wind turbine projects [7][8][9][4] and mooring lines [05, 10]. Offshore wind turbines have highlighted new needs for a better modeling of the loading [11]. Since the dynamic cable will be placed in shallower waters than in the Oil and Gas industry, it sensitivity to bio-colonization is higher. The process of bio-colonization involves the formation of residues such as algae, mussels, and oysters on the surface of the cable, often reaching several tens of centimeters in thickness. Among the organisms that can colonize dynamic cables, marine mussels are the most frequently encountered species in the wind farms in North Atlantic area [4, 12]. They are bivalve mollusks protected by two sturdy shells as shown in Figure 2. Moreover, in terms of thermal impact they are of particular interest due to their ability to filter feed on phytoplankton and sediments while searching for food, leading to significant fouling on the cable surface. Thus, biocolonization of dynamic cables by mussels has become a crucial area of research in the field of floating wind turbine technology. While the cross-linked polyethylene cable (XLPE) is the most commonly used type for dynamic cables, bio-colonization is a least understood but also can be a highly impactful factor that affects the performance and lifetime of these cables.

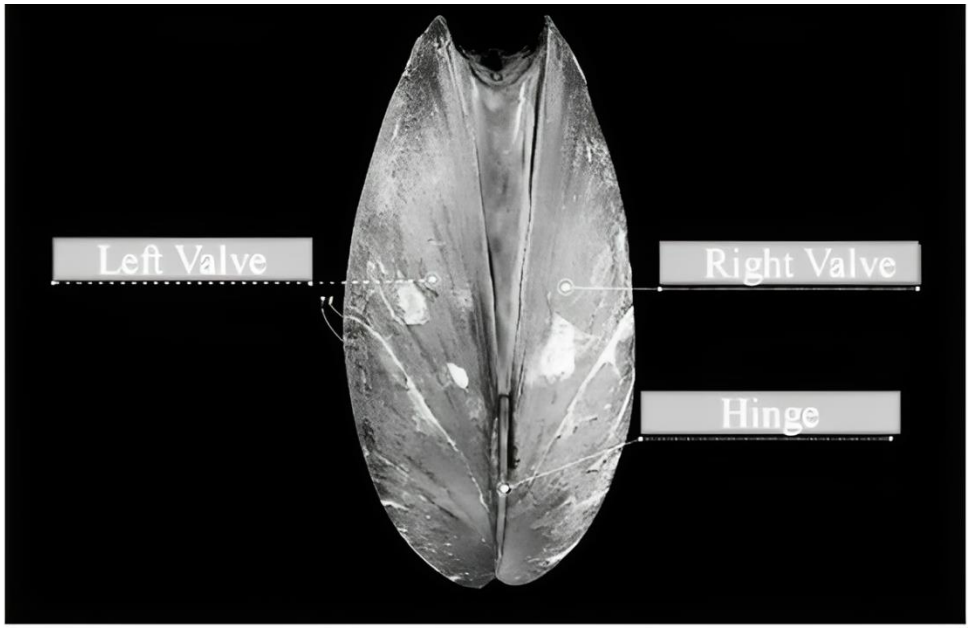

Figure 2. Mussel's anatomy.

The process of biofouling has a direct impact on the behavior of dynamic cables, as shown in Figure 3. This impact is due to several factors, including the formation of a heat shield, the addition of mass to the cable, and changes to the cable's roughness, which can affect its hydrodynamic stresses and alter its behavior during storm or fatigue situations [04, 05, 06, 11,13,14]. In addition to these factors, biocolonization has also been found to have a thermal effect on the cable, as demonstrated in studies [15] and [16].

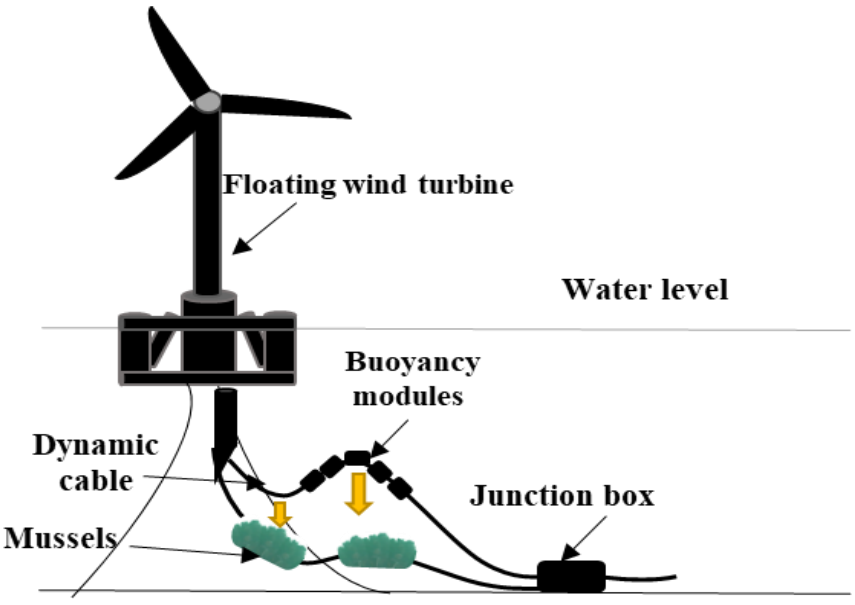

Figure 3. Impact of biofouling on the behavior of the dynamic cable.

To our knowledge, no author other Maksassi et al. [16] have conducted the thermal

characterization of mussels. They performed a thermal characterization of mussels and discovered that juvenile mussels have a higher thermal resistance than mix and adult mussels, with noting that the thermal resistance is inversely proportional to the effective thermal conductivity $\left(\frac{log\left(\frac{r_e}{r_i}\right)}{2\pi\lambda_e L}\right)$ where r_e is the external radius, r_i is the internal radius, L is the length of the sample and λ_e is the effective thermal conductivity. As a result, juvenile mussels exhibited higher thermal resistance than mix and adult mussels. The study further suggested that the conductive resistance played a dominant role in the global thermal resistance in presence of mussels. In order to fully comprehend the thermal resistance with mussels near the cable, it is crucial to identify the factors that could alter the effective thermal conductivity of mussels.

The current study aims to investigate the hypothesis proposed by Maksassi et al. [16] that juvenile mussels exhibit lower effective thermal conductivity compared to mix and adult mussels, attributed to their relatively lower natural convection existed in their pores. This study will examine the correlation between mussel porosity, temperature differential between the internal and external layers, and the effective thermal conductivity. The natural convection is influenced by the Rayleigh Number, which represents the ratio between buoyancy and viscous forces in a fluid ($Ra = \frac{\beta \Delta T \kappa D g Pr}{\nu^2}$). The Rayleigh Number is directly proportional to κ (permeability of the mussels which is proportional to the porosity), ΔT (temperature difference between the internal and external layers of the mussel cluster), β (coefficient of thermal expansion of water), D (thickness of the fluid layer), g (acceleration due to gravity), and ν (kinematic viscosity of water). This study also seeks to examine other factors that could affect the effective thermal conductivity of mussels, such as the water filtration mechanism employed by the mussels for food acquisition.

2. Porosity Measurement of Mussels and Its Effect on Effective Thermal Conductivity of Mussels

Experiments dealing with mussels for quantifying engineering impact have to represent correctly material properties: roughness, organization and porosity. The two first are available in [17] for adult mussels and the paper focusses on the third one. As previously discussed, an increase in mussel porosity results in higher effective thermal conductivity due to the associated increase in natural convection because of a higher Rayleigh number. In this section, the objective is to measure the porosity of mussels for various ages. The water displacement method is used to measure the porosity of juvenile and mix mussels. The cluster of mussels with its interstitial water (Figure 4a) is placed in a water bucket filled with water (V_W) to determine the mussel's cluster volume, which is labelled V_1, as shown in Figure 4b calculated by substituting the total volume V_T from the water volume V_W. Next, the mussels cluster is remove (Figure 4b) and placed immediately above an empty bucket to collect the interstitial water and read its volume, which is labelled V_{11} in the Figure 4c. As a result, the water porosity of a mussel's cluster is equal to $\epsilon_{mussels}=V_{11}/V_1$.

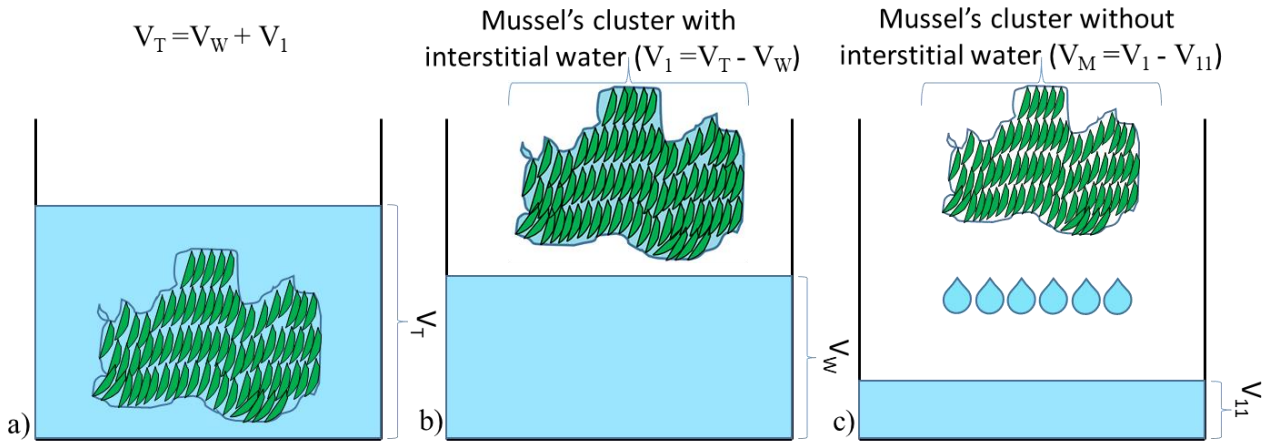

Figure 4. a) Total volume b) Water volume without mussels c) Volume of the interstitial water.

However, the water displacement method used to measure porosity in juvenile and mix mussels cannot be used for adult mussels due to their high porosity. This is because the interstitial water is difficult to measure accurately and can be lost during transfer from bucket to bucket (Figure 4b to 4c). Instead, the porosity of adult mussels will be estimated by measuring their permeability using Darcy's law and using a modified version of the Kozeny-Carman [18] equation developed by Macdonald et al [19]. This modified equation relates the particle diameter, porosity, and permeability based on a larger number of experimental data.

An experimental apparatus was developed to determine the permeability parameter, consisting of a closed circuit apparatus (shown in Figure 5) comprised of a transparent plastic tube *(Φ=110mm, L_{cyl}=1000mm)*. The setup also includes a differential pressure meter, flow meter, water valve, water pump, and water tank. Darcy's law (Equation 1)is employed to calculate the mussels' permeability.

$$\dot{Q} = \frac{-\kappa A \Delta p}{\mu L_c} \qquad (1)$$

where $\dot{Q}(m^3/s)$ is the flow rate of the fluid flowing through an area $A(m^2)$, κ is the permeability (m^2), $\Delta p(Pa) = p_a - p_b$ is the total pressure drop over the sample, $L_c(m)$ is the length between gauges, $\mu\ (Pa.s)$ is the dynamic viscosity of the fluid.

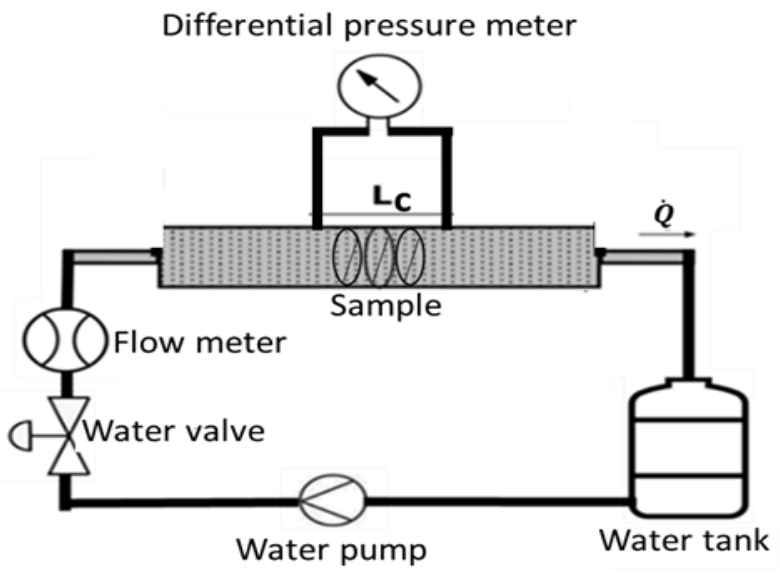

Figure 5. Experimental setup to measure the permeability.

To verify the accuracy of the permeability measurement technique, the permeability of a porous medium made of one-layer glass beads (with a diameter of 16 mm) is measured through experiments and compared to a theoretical value calculated using the modified Kozeny-Carman equation by MacDonald et al. (Equation 2). The Kozeny-Carman equation is a mathematical relationship that describes the relationship between the permeability, porosity, and specific surface area of a porous medium.

$$\kappa = \frac{d_p^2 \epsilon^3}{180(1-\epsilon)^2} \qquad (2)$$

Where d_p is the spherical particle diameter, ϵ is the volumetric void fraction (porosity). As illustrated in the Figure 6, a glass beads porous medium with a 55 % porosity is placed in the experimental setup's tube.

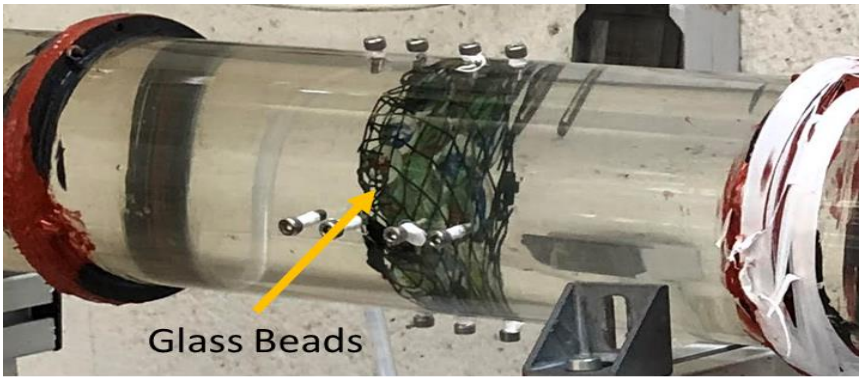

Figure 6. Glass beads in the experimental setup.

The relationship between the pressure differential (Δp) and flow rate ($\dot{Q}$) is presented in Figure 7, where it is observed that Δp increases with increasing flow rate due to their direct proportionality. The permeability of the glass bead medium is then determined using Darcy's law

and the slope of the curve in Figure 7, yielding a value of 1.168×10^{-6} m^2. The theoretical permeability value is calculated using Equation 2, with modified Kozeny-Carman constants by MacDonald et al., resulting in a $\kappa_{theoretical}$ value of 1.17×10^{-6} m^2. The small difference of 0.17 percent between the experimental and theoretical values validates the permeability measurement method.

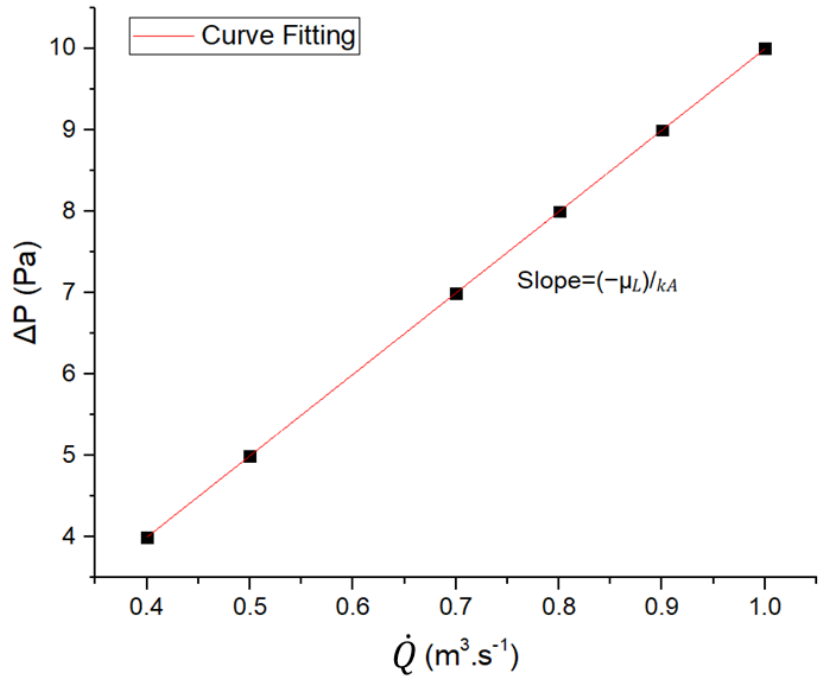

Figure 7. Pressure drop across the glass beads sample (ΔP) as function of the flow rate $\dot{Q}$.

Subsequently, the adult mussels are introduced into the experimental apparatus to determine their permeability, as illustrated in Figure 8.

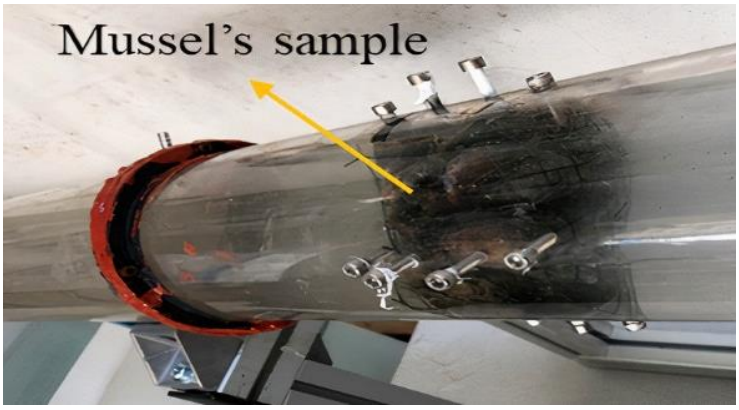

Figure 8. Adult mussels in the experimental setup.

The plot in Figure 9 displays the change in differential pressure versus flow rate for adult mussels, with the differential pressure meter having a relative uncertainty of 0.05%. As flow rate increases, the differential pressure increases proportionally. The permeability of the adult mussels is then determined using Darcy's law and the slope of Figure 9, resulting in a $\kappa_{experimental}$ value of 1.23×10^{-7} m^2. Notably, the permeability measurements were conducted solely on deceased mussels,

with the assumption that living mussels possess equivalent permeability to that of the deceased one [17].

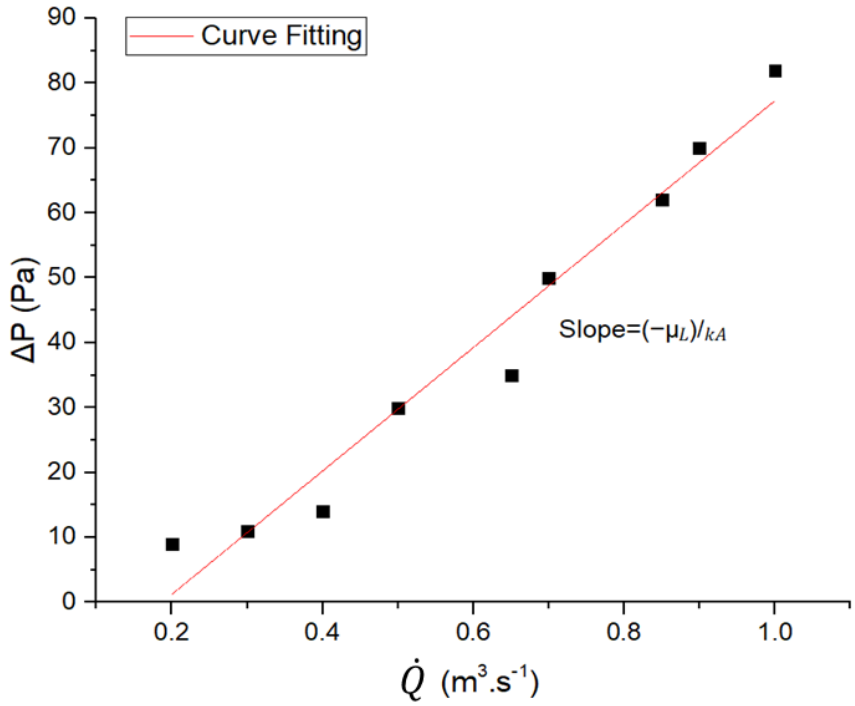

Figure 9. Pressure drop across the adult mussels sample (ΔP) as function of the flow rate $\dot{Q}$.

The porosity of the adult mussels is estimated using Equation 2, as modified by MacDonald et al to account for non-spherical particles. In this modification, the diameter term (d_p) in Equation 2 is replaced by the equivalent diameter ($d_{p,equivalent}$) for non-spherical particles, which is defined as:

$$d_{p,\,equivalent} = \epsilon . d_v \qquad (3)$$

Where d_v is the average volumetric diameter and ϵ is the sphericity of the particles. In our case, an adult mussel (12 months) specimen is typically 6 cm length and 3 cm width as shown in Figure 10. Then, its average volumetric diameter is equal to 4.24 cm and its sphericity is equal to 0.8. As a result, the adult mussels have a porosity of 22.6 %.

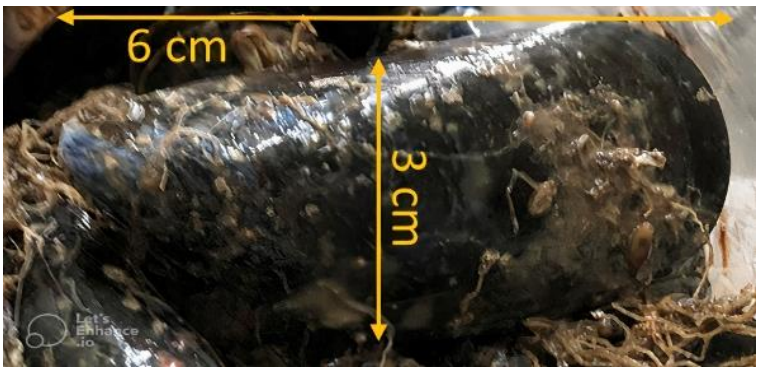

Figure 10. Size of an adult mussel's specimen.

Table 1, indicates that there is an increase in the porosity of mussels as they age. This can be attributed to the fact that the size of each mussel specimen increases with age, leading to a higher effective thermal conductivity of mussels ($\lambda_{e,biof}$). This is due to the increase in natural convection within the pores of the mussels. Consequently, the porosity of mussels plays a significant role in determining their effective thermal conductivity, as also demonstrated in Maksassi et al. [16].

Table 1. Mussel's porosity (ϵ) as well as effective thermal conductivity ($\lambda_{e,biof}$) for various ages of mussels.

Mussel's age	ϵ	$\lambda_{e,biof}$
	%	$W.m^{-1}.K^{-1}$
Juvenile (3-6 months)	15.2	4.4
Mix (juvenile and adult) (6-12 months)	18.2	8.0
Adult (12-18 months)	22.6	12.8

3. Influence of Mussel's Filtration Mechanism and Temperature Difference Between both sides of mussel Layers on Effective Thermal Conductivity of Mussels

Mussels are a type of aquatic bivalve mollusk that are renowned for their efficient filter-feeding mechanism. During the filtration process, individual mussels generate microfluidic movements, allowing them to process several milliliters of water per hour. Studies have shown that an average-sized mussel, measuring 3.4 cm in shell length, can filter up to 1.6 ml of water per hour [20]. This raises the question to check of whether the observed microfluidic movement in mussels has any impact on their effective thermal conductivity. On May 19, 2022, a measurement campaign was conducted on adult mussels that were 12 months old. The mussels were collected as patches measuring 20cm long x 15cm wide x 7cm thick in order to preserve their natural arrangement and composition, and maintain the same natural porosity. They were collected from breeding ropes located at a water depth of 4 meters at Aiguillon sur Mer (France), which is exposed to the Atlantic Ocean. After collection, the mussels were stored in buckets filled with sea water (as shown in Figure 11), and transported by car for 1 hour and 40 minutes to the LTeN laboratory, where the thermal measurements were carried out.

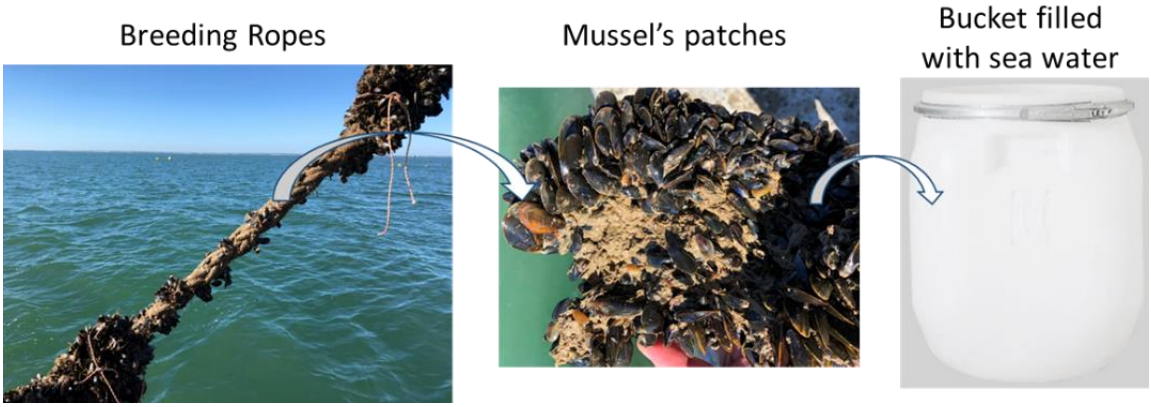

Figure 11. Mussel's patches extraction and storage.

The effective thermal conductivity was determined through a stationary measurement procedure using the same protocol as described in Maksassi et al. [16]. The experimental setup comprises an aluminum tube (ϕ_{int}=60 mm, ϕ_{ext}=70 mm, L=610 mm), which is equipped with five K-type thermocouples. Within this setup, three of the thermocouples are situated in the center of the cross-section, evenly spaced at 120° intervals, while the remaining two thermocouples are located near the ends of the tube, 5 cm from each extremity. These thermocouples are installed at grooved locations on the tube that are created using a CNC milling machine. Furthermore, the thermocouples are secured in place using a marine-grade, one-component polyurethane sealant adhesive (Sikaflex 291i). Six silicon rubber resistance tapes (610 mm x 25.4 mm) with copper etched foil (SRFGA-124/2-P from Omega) are situated on the inner surface of the aluminum tube to ensure uniform heating. A rubber air chamber used to maintain an internal pressure of approximately 1.5 bar, serves to keep the six heaters in contact with the aluminum tube and establish adiabatic boundary conditions within the tube. Furthermore, a sample holder has been fabricated to enable measurements to be taken within a tank filled with stagnant seawater. The aluminum tube is supported by a POM (polyoxymethylene) seal at each end, which is affixed using a plastic screw. These seals are mounted on a U-clamp, which is connected to a T-shaped support composed of an aluminum bar attached to a 12 mm threaded rod. Subsequently, the thermocouples and heating element cables are linked to a data acquisition system and a power supply, respectively. The data acquisition system can be used to record all measurement data, which can then be accessed using a computer and Agilent BenchLink Data Logger software.

Subsequently, the effective thermal conductivity of alive adult and dead mussels (Figure 12) is measured for different temperature differences between the both sides of the mussel layer ($\Delta T = T_1 - T_2$).

a)  b) 

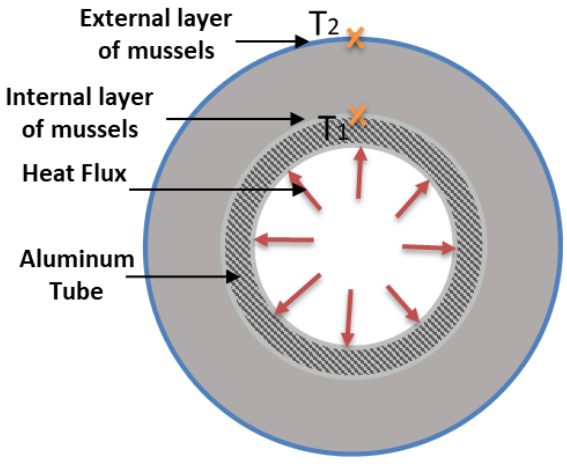

c)

Figure 12. Adult mussels (12 months) a) alive b) dead c) Central cross-section of the aluminum tube exhibiting uniform mussel's colonization.

Figure depicts the variation of the effective thermal conductivity of living and dead adult mussels as a function of the temperature difference between the both sides of the mussels' layer. The measurements were found to have a relative uncertainty of less than 9%. A repeated measurement of the effective thermal conductivity of living adult mussels at same ΔT=5.1 K is also performed, the result shows that the effective thermal conductivity is equal to 12.8 $W.m^{-1}.K^{-1}$ and 12.3 $W.m^{-1}.K^{-1}$ for measurements taken on July 8, 2020 [16] and May 19, 2022, respectively, with a difference of less than 5% between the two measurements.

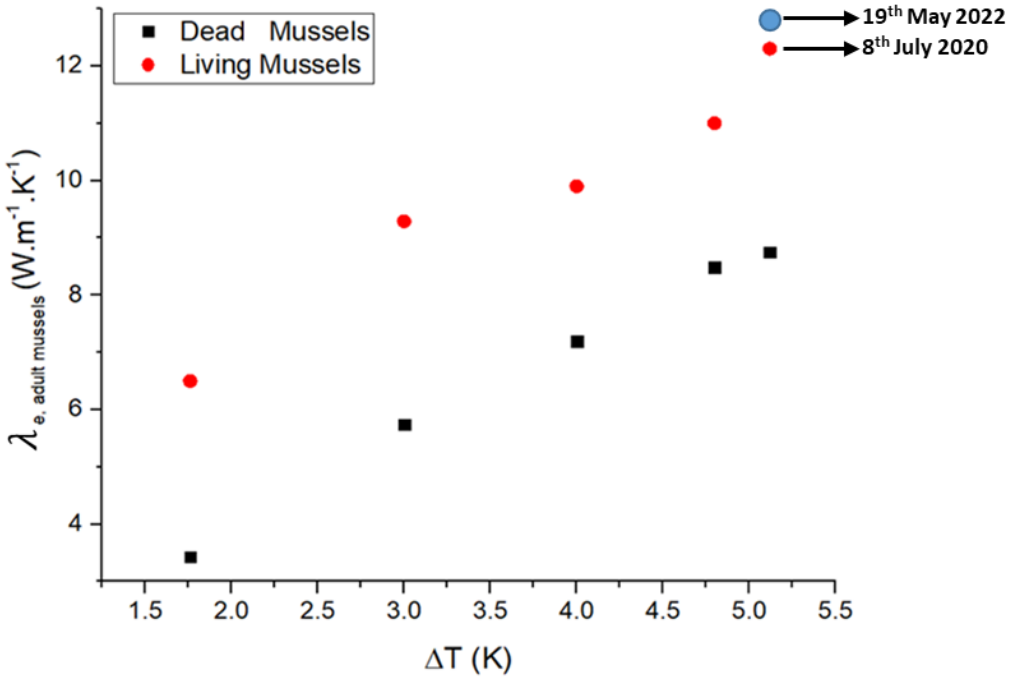

Figure 13. Effective thermal conductivity of dead and living adult mussels as function of temperature difference between the both sides of the mussels layer.

First, the effective thermal conductivity of mussels is shown to be influenced by the temperature difference (ΔT) between the both sides of the mussel layer. Figure 13 demonstrates that an increase in ΔT leads to a corresponding increase in the effective thermal conductivity of both living and dead mussels. This phenomenon attributed to the increase in the Rayleigh number (as described by Equation 2) which also increases with an increase in ΔT. The rise in Rayleigh number leads to a more developed natural convection within the fluid in the mussel pores due to density differences resulting from temperature variations between both sides of the mussel layer.

Second, at a given temperature difference (ΔT), the effective thermal conductivity of living adult mussels is significantly higher than the effective thermal conductivity of dead adult mussels (Table 2). This difference is observed to be around 3 $W.m^{-1}.K^{-1}$ on average, which corresponds to an increase about 40%. Table 2 gives the values of this relatve change as a function of ΔT. The observed difference in thermal conductivity is attributed to the fact that natural convection in the living adult mussels is bigger than in the dead adult mussels. This increased natural convection is primarily due

to the filtering mechanism of the mussels, which is only operational when they are alive.

Table 2. Effective thermal conductivity of living and dead adult mussels as function of different ΔT.

ΔT	$\lambda_{adult,living}$	$\lambda_{adult,dead}$	$\left(\frac{\lambda_{adult,living}-\lambda_{adult,dead}}{\frac{\lambda_{adult,living}+\lambda_{adult,dead}}{2}}\right)$
K	**W.m⁻¹.K⁻¹**	**W.m⁻¹.K⁻¹**	**%**
1.8	6.5	3.4	62
3	9.3	5.7	47
4	9.9	7.2	32
4.8	11	8.5	26
5.1	12.3	8.8	34

The effective conductivity of mussels is dependent on the temperature difference (ΔT), which can vary due to differences in the power levels applied to the heating elements during measurements. Therefore, in the next section, a thermal simulation will be performed using effective conductivity values estimated using a power level in a power cable that results in a copper conductor temperature of 90 degrees Celsius.

4. Juvenile and adult mussels thermal impact on copper conductor temperature of dynamic submarine electrical cable of floating offshore wind turbine

As previously demonstrated, the effective thermal conductivity of mussels is influenced by the temperature difference between both sides of the mussel layer. This effect is caused by the increased natural convection in the mussel pores, which is in turn influenced by the power applied to the heating elements during measurements. In this section to simulate the thermal effect of the mussels and check if with the presence of the mussels the copper conductor temperature will exceeds its maximum operating temperature (90 °C), the effective thermal conductivity of the mussel will be estimated by imposing a power level resulting in a dynamic cable conductor temperature of 90 °C. This value was calculated by Maksassi et al. [16] using the standards of the International Electrotechnical Commission (IEC), resulting in a power of $P_{90°C}$ = 92 W. Then, in May 2022, at power $P_{90°C}$, the effective thermal conductivity of adult mussels was measured. Due to this, adult mussels have an effective thermal conductivity of 9.1 W.m^{-1}.K^{-1} and a ΔT of 3 K which is lower than the effective thermal conductivity (12.3 W.m^{-1}.K^{-1}) measured at ΔT equal to 5.1 K.

A previous campaign provides Figures for juvenile mussels. According to measurements taken in July 2020, juvenile mussels have effective thermal conductivities of 1.6 W.m^{-1}.K^{-1} (ΔT =6 K) and 4.4 W.m^{-1}.K^{-1} (ΔT =10 K), respectively. This is determined by applying two different power levels of 40.74 W and 224 W respectively. Therefore, based on the curve fitting of two prior measurements, the effective thermal conductivity of juvenile mussels is calculated with the power $P_{90°C}$ as shown in Figure 14. Results show that the effective thermal conductivity of juvenile mussels at $P_{90°C}$ is equal to 2.45 W.m^{-1}.K^{-1} with a ΔT equal to 7.25 K.

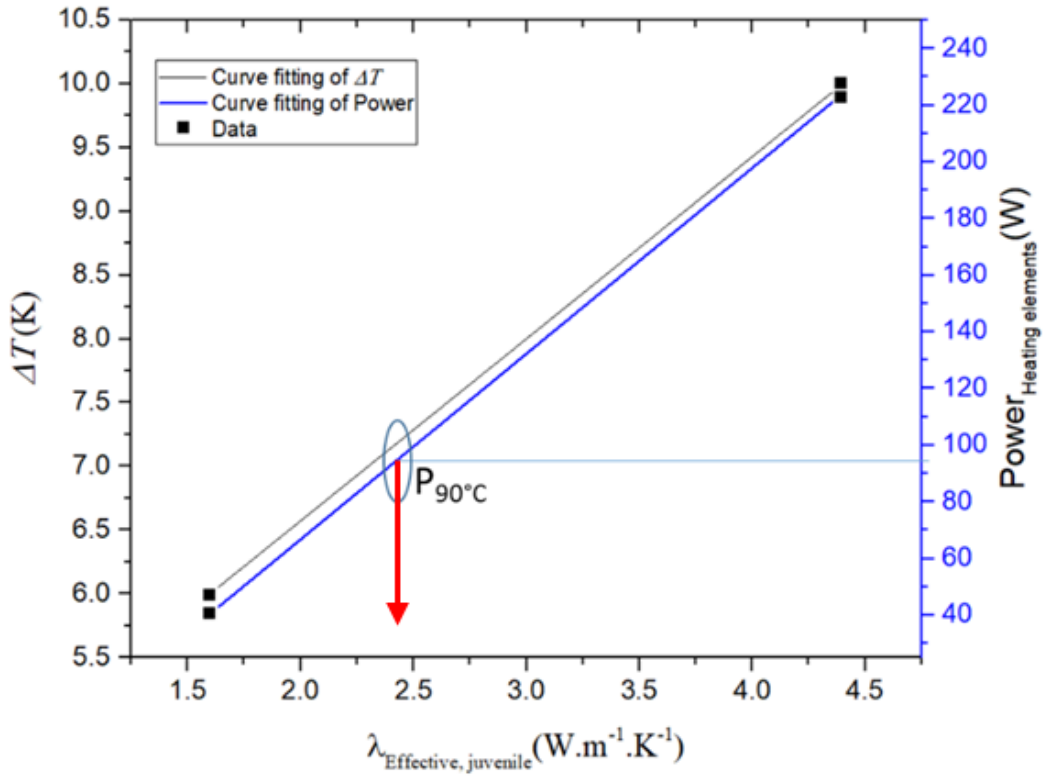

Figure 14. Effective thermal conductivity of juvenile mussels for different ΔT and imposed powers.

The effective thermal conductivity of juvenile and adult mussels, estimated at power $P_{90°C}$, is lower than that of juvenile and adult mussels, respectively, estimated at power P_1=224 W and P_2=212 W, as shown in Table 3. Hence, the thermal resistance values for juvenile (0.022 $K.W^{-1}$) and adult (0.011 $K.W^{-1}$) mussels computed at P1 and P2 are lower than those computed at $P_{90°C}$, where the values are 0.089 $K.W^{-1}$ for juveniles and 0.021 $K.W^{-1}$ for adults. The copper conductor temperature simulated with the effective thermal conductivity of the mussels estimated at $P_{90°C}$ will then be higher than the copper conductor temperature estimated at P and P_2.

Table 3. Effective thermal conductivities and thermal resistances for juvenile and adult mussels.

Mussels type	*Power*	$\lambda_{effective}$	*Thermal resistance*	*Power*	$\lambda_{effective}$	*Thermal resistance*
	W	W. $m^{-1}.K^{-1}$	$K.W^{-1}$	W	W. $m^{-1}.K^{-1}$	$K.W^{-1}$
Juvenile	92	2.45	0.089	224	4.4	0.022
Adult	92	9.1	0.021	212	12.8	0.011

Finally, the effective thermal conductivities of juvenile and adult mussels estimated at $P_{90°C}$ are used in the thermal model developed by Maksassi et al. [16] to investigate the thermal impact of mussels on the copper wire of a dynamic submarine electrical cable (20 kV, 3 × 50 mm^2 copper conductors insulated with XLPE) used in the OMDYN2 project. A two-dimensional steady-state thermal model was developed using finite elements (COMSOL software) to accurately represent the shape and materials of the cable. The model had a mesh with normal size elements of 94124 nodes in the dynamic submarine electrical cable, and was used to predict the temperature distribution within the cable.

Figure 15 shows that the copper conductor temperature is 95.18 °C for juvenile mussels and 90.8 °C for adult mussels colonized around the dynamic cable, which is higher than the IEC standard maximum operating temperature of 90 °C [21].

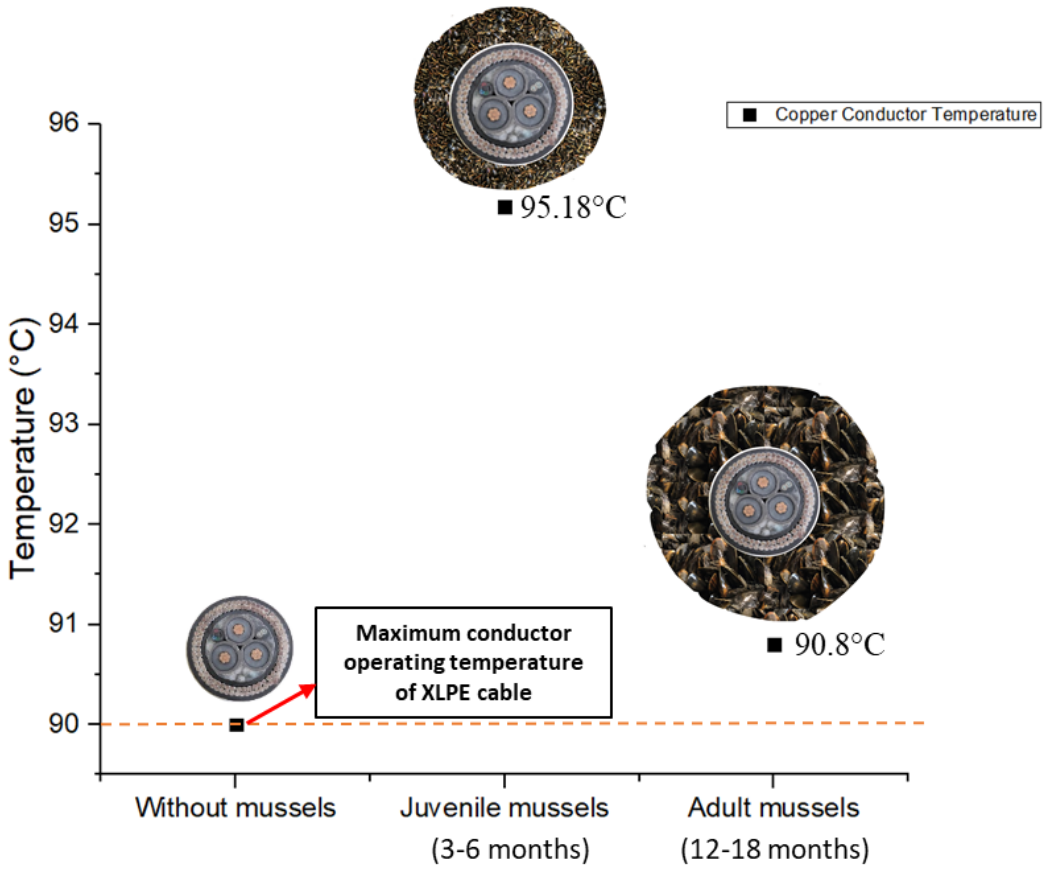

Figure 15. Copper conductor temperature of XLPE DSEC with and without mussels.

As expected, the copper conductor temperature simulated with the effective thermal conductivity of mussels estimated at $P_{90°C}$ is higher than those estimated at P_1 and P_2 due to the higher thermal resistance in the case of the effective thermal conductivity estimate at $P_{90°C}$ (Table 4).

Table 4. Effective thermal conductivities and thermal resistances for juvenile and adult mussels.

Mussel's type	*Power*	*Copper conductor temperature*	*Power*	*Copper conductor temperature*
	W	°C	W	°C
Juvenile	92	95.18	224	91.3
Adult	92	90.8	212	89.1

It is important to note that the expected lifetime of XLPE is between 40 and 60 years at the rated operating temperature of 90 °C. However, for rated operating temperatures between 95 and 105 °C, this lifetime range can be reduced to between 7 and 30 years [22]. As a result, the presence

of mussels has a thermal effect on the DSEC conductor temperature, particularly on juvenile mussels, where the conductor temperature of the cable reaches 95.18 °C. It should be noted that all thermal modeling examples regarding the thermal impact of mussels on dynamic electrical cables rely on the assumption that the water surrounding the mussels is stationary, as a worst-case scenario. In future work, the influence of water currents passing over the mussels will be considered.

5. Conclusion

Understanding the thermal properties of biocolonization on dynamic cables can lead to significant improvements in cable design and maintenance. Accurately assessing the thermal impact of biocolonization, particularly from mussels, can help prevent cable damage and increase the lifespan of the cables, resulting in a more sustainable and cost-effective solution for offshore wind farms. Furthermore, advancing cable design based on this understanding can lead to the development of more robust and resilient cables that can withstand the harsh marine environment, ultimately improving the overall performance of floating wind turbines.
The measurement of the thermal properties of this natural medium (biofouling) is rarely addressed in the marine energy literature. The thermal characterization of mussels was carried out in stagnant water. The effective thermal conductivity of adult mussels was measured when the mussels are alive and when they are dead. Results shows that the effective thermal conductivity of adult alive mussels is higher than the effective thermal conductivity of adult dead mussels due to the water filtering effect which creates an additional micro-movement increasing the effective thermal conductivity of the mussels. On the other hand, the effective thermal conductivity of the mussels increases with the increasing of the temperature difference between both sides of the mussel layer due to natural convection phenomenon. The porosity of various ages of mussels is measured and shows that the porosity of the juvenile mussels is the smallest comparing to mix and adult mussels respectively. This confirms why the juvenile mussels has the lowest effective thermal conductivity (meaning highest thermal resistance) comparing to mix and adult mussels. It has been proven that the effective thermal conductivity of mussels is affected by three factors: the water porosity, the temperature difference between their internal and external layer and their filtering phenomenon (nutrition). While the water current effect on the effective thermal conductivity must be studied in future work.

The investigation reveals that the biofouling of mussels causes an elevation in the temperature of the copper conductor of the dynamic electrical cable beyond its permissible limit of 90°C. This temperature increase depends on the age of mussels and their associated thermal resistance. Juvenile mussels exert a bigger thermal impact on the copper conductor temperature of the dynamic electrical cable compared to mixed and adult mussels, resulting in a rise in the temperature of the copper conductor of the cable up to 95.18 °C. This elevated temperature of the copper conductor reduces the lifetime of the XLPE insulation, the overall fatigue lifetime of the cable and increases maintenance costs. Notably, all simulations assume the surrounding water to be stagnant.

This study is a significant step forward in our understanding of the thermal behavior of mussels and its impact on the performance of submarine dynamic electrical cables. This can result in the development of improved cable designs and maintenance protocols, making them more durable and efficient in the long run. This study holds great promise for the advancement of floating wind turbine technology and the wider field of underwater cable design and maintenance.

Acknowledgments: This work was carried out within the framework of the OMDYN2 project (funding from France Energies Marines as well as the French National Research Agency under the Investments for the Future program bearing the reference ANR-10-IEED-0006-28) and the BIODYTHERM project (funding from WEAMEC, West Atlantic Marine Energy Community, and with support from the Pays de la Loire Region. The authors also like to thank Arnaud ARRIVE (for the technical realizations) for his assistance in the fabrication of the experimental tubes.

References

1. Schoefs F., Oumouni M., Ahmadivala M., Bourget S., Luxcey N., Guerin P., Dupriez-Robin F., "Unified system analysis for time variant reliability of a floating offshore substation", JMSE, 'SI: Safety and Reliability of Offshore Energy Facilities', in press. 2023.
2. Schoefs F., "Dynamic power cables facing marine growth: quan8fying the effects for design and monitoring", FOWT 2023, "Mooring lines & Power cables panel: How to analyze and safeguard the integrity of subsea lines and cables", May 11th, May 10-12th 2023, La Cité Nantes Congress Centre, Nantes, France.
3. Marty A., Schoefs F., Soulard T., Berhaul, C., Facq J-V., Gaurier B., Germain G., "Effect of roughness of mussels on cylinder forces from a realistic shape modelling", Journal of Marine Science and Engineering, section Ocean Engineering, Volume 9, Issue 6, # 558, doi.org/10.3390/jmse9060598, 2021
4. Marty A., Berhault, C., Damblans G., Facq J-V., Gaurier B., Germain G., Soulard T., Schoefs F., "Experimental study of marine growth effect on the hydrodynamical behaviour of a submarine cable", Applied Ocean Research, 114 (Sept. 2021), #102810, doi.org/10.1016/j.apor.2021.102810, 2021
5. Marty, A., Schoefs F., Damblans G., C., Facq, J-V., Gaurier, B., Germain, G., "Experimental comparative study of two kinds of hard marine growth effects on the hydrodynamical behaviour of a cylinder submitted to wave and current solicitations.", Ocean Engineering, Volume 263, 1 November 2022, doi.org/10.1016/j.oceaneng.2022.112194 – 2022
6. Zeinoddini M., Bakhtiari A., Schoefs F., Zandi A. P., "Towards an Understanding of the Marine Fouling Effects on VIV of Circular Cylinders: Partial Coverage Issue", Biofouling, 33:3, 268-280, doi: 10.1080/08927014.2017.1291803 – 2017.
7. Heaf, N.J. The Effect of Marine Growth on The Performance of Fixed Offshore Platforms in The North Sea. In Proceedings of the Offshore Technology Conference, Houston, TX, USA, 30 April–3 May 1979; p. 14, doi:10.4043/3386-MS.
8. Jusoh, I.; Wolfram, J. Effects of marine growth and hydrodynamic loading on offshore structures. J. Mek. 1996, 1, 77–98.
9. Schoefs, F., Boukinda, M.L. Sensitivity Approach for Modeling Stochastic Field of Keulegan–Carpenter and Reynolds Numbers Through a Matrix Response Surface. J. Offshore Mech. Arct. Eng. 2010, 132, 011602, doi:10.1115/1.3160386.
10. Schoefs F., Bakhtiari A., Ameryoun H. "Evaluating of hydrodynamic force coefficients in presence of biofouling on marine/offshore structures, a review and new approach", Journal of Marine Science and Engineering, section Ocean Engineering / Fluid/Structure Interactions II, 10(5), 558, https://doi.org/10.3390/jmse10050558– 2022
11. Maduka M., Schoefs F., Thiagarajan K., Bates A., "Hydrodynamic effects of biofouling-induced surface roughness – Review and research gaps for shallow water offshore wind energy structure", Ocean Engineering, 272(15/March 2023), 113798, https://doi.org/10.1016/j.oceaneng.2023.113798 – 2023
12. Decurey B., Schoefs F., Barillé A.L., and Soulard T., "Model of Bio-Colonisation on Mooring Lines: Updating Strategy based on a Static Qualifying Sea State for Floating Wind Turbines", Journal of Marine Science and Engineering, Section Ocean Engineering, Special Issues

"Monitoring of Coastal and Offshore Structures", Published on line: 11 FEV 2020, 8:108, doi.org/ 10.3390/jmse8020108 – 2020
13. Ameryoun A., Schoefs F., Barillé L. Thomas Y., "Stochastic modeling of forces on jacket-type offshore structures colonized by marine growth", Journal of Marine Science and Engineering, section Ocean Engineering, Marine Structures, 7(5), 158, https://doi.org/10.3390/jmse7050158 – 2019
14. Spraul, C., Pham, H., Arnal, V., & Reynaud, M. (2017, August). Effect of Marine Growth on Floating Wind Turbines Mooring Lines Responses. In AFM 2017 23ème Congrès Français de Mécanique.
15. Matine A., Schaeffer E., Bonnard C-H. Investigation of the biofouling thermal effects on offshore wind turbine power cables. 10th International Conference on Insulated Power Cables (Jicable'19), Session B9 Submarine cables current rating, Topic 9: Submarine Cable Systems (AC & DC), 23-27 June 2019, Paris Versailles, France.
16. Maksassi, Z.; Garnier, B.; Moctar, A.O.E.; Schoefs, F.; Schaeffer, E. Thermal Characterization and Thermal Effect Assessment of Biofouling around a Dynamic Submarine Electrical Cable. *Energies* **2022**, *15*, 3087. https://doi.org/10.3390/en15093087
17. Schoefs F., O'Byrne M., Pakrashi V., Gosh B., Oumouni M., Soulard T., Reynaud M., "Fractal Dimension as an Effective Feature for Characterizing Hard Marine Growth Roughness from Underwater Image Processing in Controlled and Uncontrolled Image Environments", Journal of Marine Science and Engineering, 2021, 9(12), 1344; doi.org/10.3390/jmse9121344 – 2021
18. M. Rahrah, L. A. Lopez-Peña, F. Vermolen, and B. Meulenbroek, "Network-inspired versus Kozeny–Carman based permeability-porosity relations applied to Biot's poroelasticity model," *J.Math.Industry*, vol. 10, no. 1, p. 19, Dec. 2020, doi: 10.1186/s13362-020-00087-z.
19. M. J. MacDonald, C.-F. Chu, P. P. Guilloit, and K. M. Ng, "A generalized Blake-Kozeny equation for multisized spherical particles," *AIChE J.*, vol. 37, no. 10, pp. 1583–1588, Oct. 1991, doi: 10.1002/aic.690371016.
20. L. A. van Duren, P. M. J. Herman, A. J. J. Sandee, and C. H. R. Heip, "Effects of mussel filtering activity on boundary layer structure," *Journal of Sea Research*, vol. 55, no. 1, pp. 3–14, Jan. 2006, doi: 10.1016/j.seares.2005.08.001.
21. [IEC] The International Electroctechnical Comission. Electric cables – Calculation of the current rating, Thermal resistance – Calculation of thermal resistance. *IEC 60287-2,* 2015.
22. A. S. Alghamdi and R. K. Desuqi, "A study of expected lifetime of XLPE insulation cables working at elevated temperatures by applying accelerated thermal ageing," *Heliyon*, vol. 6, no. 1, p. e03120, Jan. 2020, doi: 10.1016/j.heliyon.2019.e03120.